

Corrosion resistance studies on grain-boundary etched drug-eluting stents

Ralf Rettig · Julia Kunze · Michael Stöver ·
Erich Wintermantel · Sannakaisa Virtanen

Received: 20 December 2005 / Accepted: 7 April 2006 / Published online: 3 February 2007
© Springer Science+Business Media, LLC 2007

Abstract In this paper we compare the influence of different microstructures on the corrosion resistance of new drug-eluting stainless steel stents, which have been produced by grain-boundary-selective electrochemical etching processes. The morphology of the stent surfaces was analysed by scanning electron microscopy (SEM), and the surface composition was investigated with Auger electron spectroscopy (AES) as well as with energy dispersive X-ray analysis (EDX). The passivity of the different microstructured stents was studied by cyclovoltammetry in Ringer solution. Release of nickel and chromium was assessed after potentiostatic experiments in Ringer solution by analysing the collected electrolyte with AAS. For stents produced by different two-step etching procedures bringing about ideal morphologies regarding the mechanical and biological properties of the surface, no significant differences in the passivation behaviour could be observed. A two-step process using first nitric acid and oxalic acid in a second step produces stent surfaces with very good corrosion properties: electrochemical analysis shows that the range of stable passivity is the same as for conventional stent surfaces,

and low rates of nickel and chromium release are observed. The etching procedures do not seem to change the surface oxide layer composition.

Introduction

Cardiovascular diseases are the leading cause of death in many countries [1]. Stenting is an upcoming surgical technique for treating stenosis but further improvements are still under investigation [2]. Coronary stenting has reduced the restenosis rate in comparison to balloon angioplasty. The studies in references [3, 4] give a restenosis rate of 30% and 59% for the studied balloon angioplasty treatments, whereas other investigations [5, 6] show a restenosis rate of 25% and 37% for the examined stented lesions. Stenosis is the closure of a vessel due to arteriosclerotic disease. As mentioned, in several cases the vessel closes again some time after treatment, this means restenosis occurs. The restenosis rate is variable and depends among others on coronary lesion characteristics and patient demographics [7]. Coating the stents with drugs that are inhibiting the main factor for restenosis, the neointimal proliferation, can further reduce the still unacceptably high rate. Several drugs are currently under investigation; one of them is Rapamycin/Sirolimus [8]. A common approach for local drug delivery systems on stents is the use of polymer carrier layers, which show controllable release kinetics. For this purpose drug-free polymers are blended with Sirolimus and covered with a second polymer layer, which controls drugs release [9]. The application of the polymer coatings on

R. Rettig · J. Kunze (✉) · S. Virtanen
Institute for Corrosion and Surface Science (LKO),
Department of Materials Science, University of Erlangen-
Nuremberg, Martensstr. 7, 91058 Erlangen, Germany
e-mail: kunze@ww.uni-erlangen.de

M. Stöver · E. Wintermantel
Central Institute for Medical Engineering, Technical
University of Munich, Boltzmannstr. 11, 85748 Garching,
Germany

stents is challenging and there is the risk that the layers can spall from the surface due to mechanical strains [10]. Additionally there is the risk of late side effects such as late restenosis and late thrombosis. An alternative possibility for drug-releasing systems on stents is to perform direct coating of microstructured surfaces. Microstructuring leads to a large surface area and hence provides a big depot volume. It has been shown that Rapamycin can adhere to such surfaces and that those systems have controllable release kinetics [10]. Selective electrochemical grain-boundary etching of stainless steel that has originally been developed for metallographic purposes [11] has been demonstrated to produce microstructures that are very well suited for drug coating [10]. Nevertheless, for biomedical applications the corrosion resistance of the stents surfaces must be elucidated. This is of special importance in the case of stents produced of surgical grade stainless steels, since stainless steels as such are known to be susceptible to local corrosion effects in chloride containing environment (see e.g. [12, 13]). Moreover, the etching process changes the surface morphology and eventually the surface chemistry and both these factors may influence the corrosion behaviour of the substrate. Therefore, in the present work, the surface morphology and the chemical composition of the oxide layer were analysed. In-vitro corrosion experiments were performed in simulated body solution (Ringer's physiological solution). The objective of the present paper is to investigate the corrosion resistance of selectively grain-boundary etched stainless steel stents (316L) and to obtain information on the influence of the etching process on the morphology and the chemical composition of the stent surface. This knowledge will then lead to an optimisation of the etching process for the improvement of the stenting technique.

Experimental section

Reagents, solutions and electrode materials

As samples for all experiments standard translumina® Yukon stents were used (translumina GmbH, D-80538 Munich, Germany) having 12 mm length, 140 µm wall strut thickness and 120 µm strut width. They are made from stainless steel 316L and routinely electropolished prior to every further surface treatment. The grain-boundary etching process performed with the stents as anode and a stainless steel cathode is explained in detail in [10, 11]. For each etching method differently strong etchings were performed, for all etching strengths one new as-fabricated, i.e. electropolished

stent was used. The current is applied by a DC-transformer (PPS 3003 from Conrad, D-92240 Hirschau, Germany), current and etching time are adjustable parameters. In this work the influence of different etching solutions on the surface structure and its chemical nature is elucidated. The focus lies on two-step processes. In the first step, etching is performed in nitric acid (40%, p.a., Merck GmbH, D-64293 Darmstadt, Germany), after cleaning the stent a second etching process is run in a different electrolyte being hydrochloric acid (24%, p.a.), oxalic acid (10%, p.a.) or phosphoric acid (85%, p.a., all from Merck KGaA, D-64293 Darmstadt, Germany).

The corrosion resistance of the stents was investigated in Ringer solution. The composition of this electrolyte solution is given in Table 1 with all chemicals having p.a. grade (NaCl, KCl, MgSO₄ · 7H₂O from Merck KGaA, D-64293 Darmstadt, Germany; CaCl₂ · 2H₂O, NaH₂PO₄ · H₂O, NaHCO₃, C₆H₁₂O₆ from Sigma-Aldrich Chemie GmbH, D-89555 Steinheim, Germany).

Prior to all experiments the glassware was cleaned in Carot acid (1:3 mixture of H₂O₂ and H₂SO₄) and thoroughly rinsed with Milli-Q water (resistivity 18.2 MΩcm). All aqueous solutions were prepared from ultra pure water purified by a Milli-Q-water system having a resistivity of 18.2 MΩcm. For cyclic voltammetry all electrolyte solutions were deaerated by purging with nitrogen (>99.999% nitrogen, Linde AG, D-82049 Höllriegelskreuth, Germany) for at least 40 min before starting the experiments, a nitrogen blanket was maintained over the solution throughout the experiment. The electrochemical measurements were performed with a three-electrode-set-up in Ringer solution. The counter electrode was a platinum sheet and a saturated Ag/AgCl-electrode with a potential of 220 mV_{SHE} was used as reference electrode. In this paper all potentials are referred to the Ag/AgCl scale.

Table 1 Composition of the Ringer solution used in the electrochemical experiments

Ion	Molar concentration/10 ⁻³ mol/L
Na ⁺	143
K ⁺	5.4
Ca ²⁺	1.8
Mg ²⁺	0.8
Cl ⁻	125
SO ₄ ²⁻	0.8
H ₂ PO ₄ ⁻	1.0
HCO ₃ ⁻	26
C ₆ H ₁₂ O ₆	5.5
Total	310

Electrochemical measurements and instrumentation

For each etching method differently strong etched stents were produced and analysed by electrochemical measurements. For nitric acid and nitric/oxalic acid, a lightly and a strongly etched stent were used; for nitric/hydrochloric acid a lightly, a medium and a strongly etched stent and for nitric/phosphoric acid only a lightly etched stent were used. From the electropolished and sandblasted reference stents two of each were analysed. All measurements were carried out at room temperature. The electrochemical experiments were performed using a computer controlled system consisting of a potentiostat/galvanostat Jaisle 1030DA (from Jaisle Elektronik GmbH, D-71336 Waiblingen, Germany), connected to a digital multimeter (Keithley 199, from Keithley Instruments Inc., Cleveland, Ohio 44139, USA) interfaced to a computer. Data acquisition was performed via in-house software. A computer controlled the potential with a function generator (Prodis 1/16I from ASM GmbH, D-85452 Moosinning, Germany). Before starting the experiment, the open circuit potential of the respective stents was determined in the same apparatus. The cyclovoltammetric experiments were started after at least 45 min when the open circuit potential remained stable. The limits of the scans were chosen to a cathodic potential of $E = -1050$ mV and an anodic potential of 1200 mV, starting at the open circuit potential. The scan rate was 1 mV/s in all experiments. The respective stent was connected as working electrode.

For the in-vitro corrosion resistance measurements the same three-electrode-set-up was used as for cyclovoltammetry. In order to get sufficiently high concentrations of heavy metal ions in the electrolyte a much smaller cell was chosen. The cell volume was approximately 50 ml compared to the cell volume for the cyclovoltammetric experiments with 500 ml. The measurements of in-vitro corrosion resistance were carried out in solutions open to air. The stent was placed in Ringer solution for 72 h at a constant potential that was 150 mV above the breakthrough potential. In the corrosion resistance studies, one stent was corroded for each etching method.

Surface characterization

For scanning electron microscopy (SEM) a Hitachi FE 4800 including an EDX-analyser (energy dispersive X-ray analysis) EDAX Genesis was used (Hitachi High-Technologies Europe GmbH, D-47807 Krefeld, Germany). The SEM pictures were taken with an acceler-

ation voltage of 10 kV and a current of 10 μ A, for EDX-analysis 20 kV and 20 μ A were used. In order to get sufficient statistics, for each etching procedure at least two identically treated stents were analysed by EDX. On these stents several point analyses were conducted. In sum for each etching method at least five measurements were done for the grain boundaries, and at least six for the grain centres at different positions. On the electropolished stents two EDX measurements were done, on the sandblasted ones seven measurements. The results of the EDX-measurements were achieved by calculating mean values and single standard deviations from the measurements.

Auger spectroscopy was performed with a PHI 670 Auger electron spectrometer (AES, Physical Electronics GmbH, D-85737 Ismaning, Germany). The fits for quantitative analysis were done with an internal database of the fitting software. Auger analysis was conducted on one etched stent for each etching method. On the electropolished stent five point measurements were made and on the stent etched with nitric/oxalic acid four measurements were done for the grain boundaries and three for the grain centres. These measurements allow a statistical analysis. The later given values for Auger analysis are mean values with their single standard deviations.

Atomic absorption spectrometry

The atomic absorption spectrometry (AAS) was performed with the flame AAS technique (AAS “Varian Spectra A-40” from Varian Deutschland GmbH, D-64289 Darmstadt, Germany) for all detected chromium, nickel and iron quantities if their values were above 0.5 mg/L. Otherwise the analysis for chromium and iron was performed with a graphite furnace AAS (Perkin Elmer Analyst 800, PerkinElmer LAS (Germany) GmbH, D-63110 Rodgau-Jügesheim, Germany, detection limit 0.002 mg/L). One sample was analysed for each etching method.

Results

Surface morphology of the stents

The scanning electron microscope (SEM) pictures of Fig. 1 show the influence of the different surface treatments on the morphology of the stent surfaces. The second etching procedure influences the surface morphology of the stents in different ways depending on the nature of the electrolyte. Figure 1 shows stents treated in the different electrolytes; they have been

electropolished (Fig. 1a), sandblasted (Fig. 1b), etched with nitric acid (Fig. 1c), etched first with nitric acid followed by oxalic acid (Fig. 1d), followed by phosphoric acid (Fig. 1e) and followed by hydrochloric acid (Fig. 1f). As the electropolished and the sandblasted stents (Fig. 1a, b) do not show a grain boundary structure, they are used as references in all experiments. The electropolished stent (Fig. 1a) shows nearly no holes and has a completely homogeneous and flat surface. In contrast to this the surface of the sandblasted stent is very rough and inhomogeneous and shows small particles that are left from the sandblasting process. The surface does not show any regular structure. The different electrolytes used for etching lead to quite different surface morphologies. Fig. 1c depicts the morphology of a stent surface that was etched in nitric acid only. It shows very deep grain-boundary trenches, the edges are well visible and clearly separated by flat walls, and the grain centres are smooth. Additionally some conical holes with even walls can be seen. A two-step etching process with nitric acid/oxalic acid leads to the morphology depicted in Fig. 1d. The grain boundary trenches are not as deep as those present after a nitric acid treatment. The trenches have a scaly morphology and the grain centres have a slightly rougher

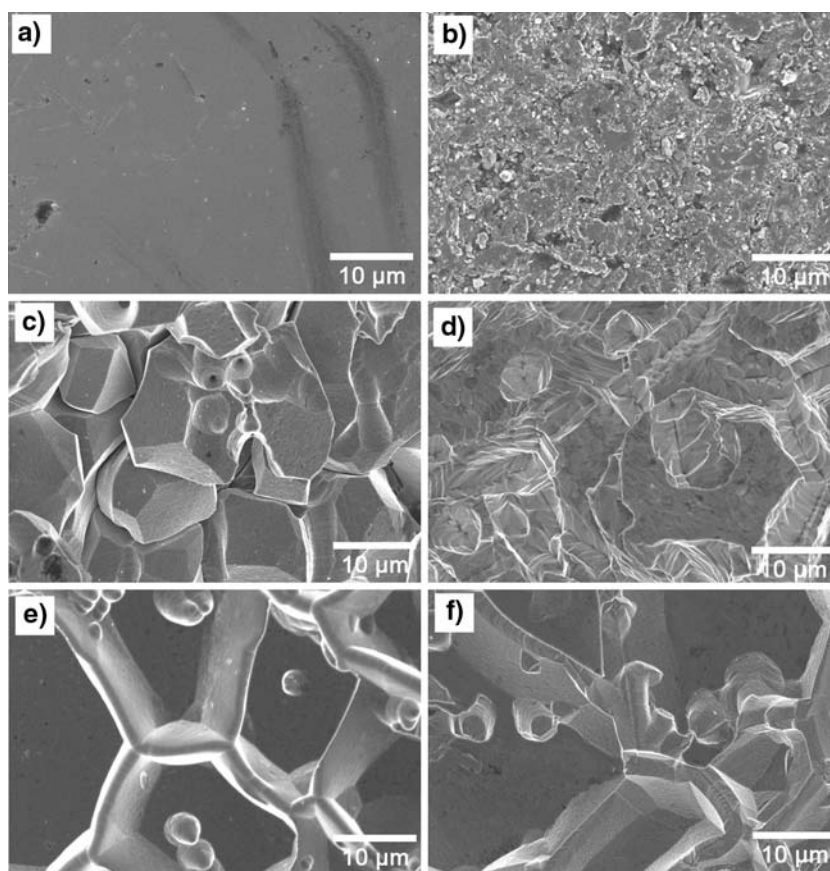
surface. There are some holes visible that show a similar scaly structure as the grain boundaries, but they are not conical as those visible on the surface in Fig. 1c. Another two-step process was performed with nitric acid/phosphoric acid (Fig. 1e). After this etching, the grain-boundaries have deep trenches with even edges but these are not as sharp as those obtained after the simple nitric acid treatment. Some conical holes can be seen. Two-step etching with nitric acid / hydrochloric acid was also examined (Fig. 1f). The surface is characterised by large grains with smooth grain centres, separated by deep trenches, which have even but sharp edges. All surfaces show small holes.

Chemical composition of the stents

EDX

The surface composition was analysed using energy disperse X-ray analysis (EDX). Due to the information depth of some microns, only in case of thicker corrosion layers results can be expected to differ from these of the substrate material. The deep and sharp grain-boundaries are very difficult to examine with EDX as some of the escaping X-rays get absorbed in

Fig. 1 (a–f): SEM pictures of etched stents: electropolished (a), sandblasted (b), etched with nitric acid (c), etched with nitric acid and secondly with oxalic acid (d), secondly with phosphoric acid (e), secondly with hydrochloric acid (f)



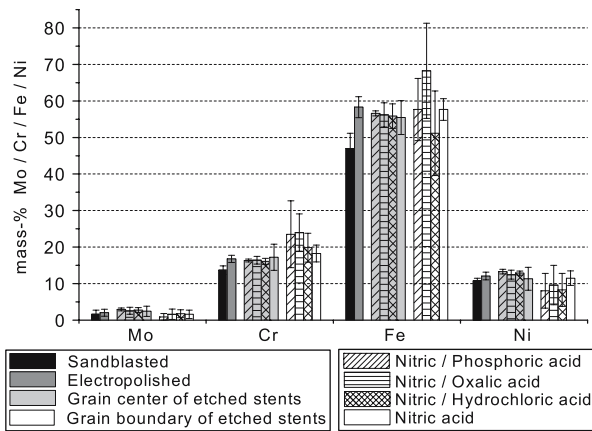


Fig. 2 EDX data of surface composition of stents etched in nitric and secondly in phosphoric acid (diagonally hatched columns), nitric and oxalic acid (horizontally hatched columns), nitric and hydrochloric acid (cross-hatched columns) and only in nitric acid (empty columns). As reference, results for sandblasted (black columns) and electropolished stents (dark grey columns) are given. Values for grain centres are given in light grey columns and values for grain-boundaries are given in white columns. The graph shows mean values and single standard deviations

the walls of the grain boundaries (edge effects). The graph in Fig. 2 depicts the results obtained by EDX analysis. No remarkable differences could be observed in the composition of the stents etched with different etching rates, and thus different dissolution rates and differently strong material removal. The graph shows the mean values and the standard deviation of the measurements for all etching rates (in mass %) of the important elements of the steel at the grain centre and at the grain-boundaries. The different columns represent the respective etching solution. For each analysed element (Mo, Cr, Fe, Ni) the composition of the electropolished and the sandblasted stents are given as references. The statistics show that there is no significant difference between the contribution of the grain centres of all stents and the references because the values are quite similar and the standard deviation is small. In contrast to this, the measured composition of grain boundaries shows a larger standard deviation and the values are different for differently treated stents.

Auger electron spectroscopy

For an analysis of the surface oxide layer composition it is advantageous to use Auger electron spectroscopy (AES), as this technique is surface sensitive with an information depth of some nanometers. In contrast to EDX it is therefore possible to analyse very thin passive layers. As we could not detect a thick corrosion product layer on the etched material, this method is

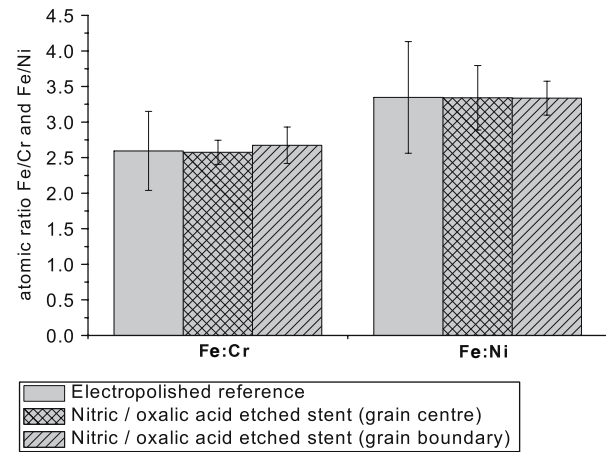
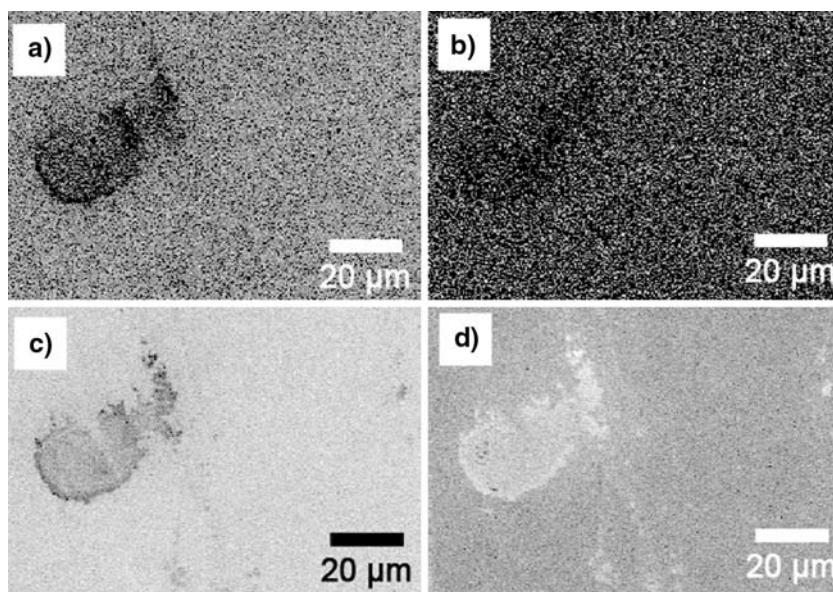


Fig. 3 Atomic ratios of the main alloying elements in 316L measured with AES showing the surface composition of different stents. Given are Fe/Cr and Fe/Ni ratios for electropolished reference (empty grey columns), grain centre (cross-hatched columns) and grain boundary (diagonally hatched columns) of a stent etched in nitric and oxalic acid. The graph shows mean values and single standard deviations

able to give further hints for the surface composition. Fig. 3 shows the mean values and the standard deviation of the atomic ratio of iron relative to chromium (Fe/Cr) and of iron relative to nickel (Fe/Ni). An electropolished sample was used as a reference for the AES measurements (empty grey column, Fig. 3). We limited the surface examination to its most important alloying elements, iron, nickel and chromium. A stent etched in a two-step process with nitric acid/oxalic acid (columns with cross-hatched and diagonal lines) was assessed in the same way and compared to the reference stent. The Fe/Cr-ratio is nearly the same for the reference sample and the examined stent that was etched with oxalic acid in a second step. This can also be seen for the Fe/Ni-ratio. As AES is extremely surface sensitive, the measured atomic ratios are representative for the chemical composition of the oxide layer on the stent surface. The ratio of iron-to-nickel is found to be 3.3 (the bulk alloy 316L has a Fe/Ni-ratio of 5.1) and the iron-to-chromium-ratio is measured to 2.6 (316L has a Fe/Cr-ratio of 3.1). The standard deviations are largest for the electropolished stent.

Additionally, Auger mappings were acquired for the electropolished stent and the stent etched in nitric acid followed by oxalic acid. Fig. 4 shows AES mappings of the electropolished stent that depict a completely homogenous surface. The spot on the left half of the picture is assigned to some contamination on the surface (Fig. 4a, c, d). Our analysis of the electropolished stent does not show any variation in its chemical

Fig. 4 (a–d): AES mapping of an electropolished stent with the distribution of the elements iron (a), nickel (b), oxygen (c) and carbon (d). Areas with high concentrations are black and with low concentrations are white in the pictures



composition as it can be seen in the AES mapping (Fig. 4a–d) and it is therefore used as a reference for the Auger experiments.

Figure 5 shows the surface composition of stents etched in nitric acid followed by oxalic acid. The distribution of nickel seems to be regular all over the surface of the stent (Fig. 5b), whereas all other elements show a variation in content, which reflects the grain boundary structure of the stent (Fig. 5b–d). This structure visible in the AES mappings is most likely due to topographic effects caused by the edges of the grain boundaries. The edges of the deep grain boundaries lead to an absorption of emitted Auger-electrons, which is visible in the mappings. This

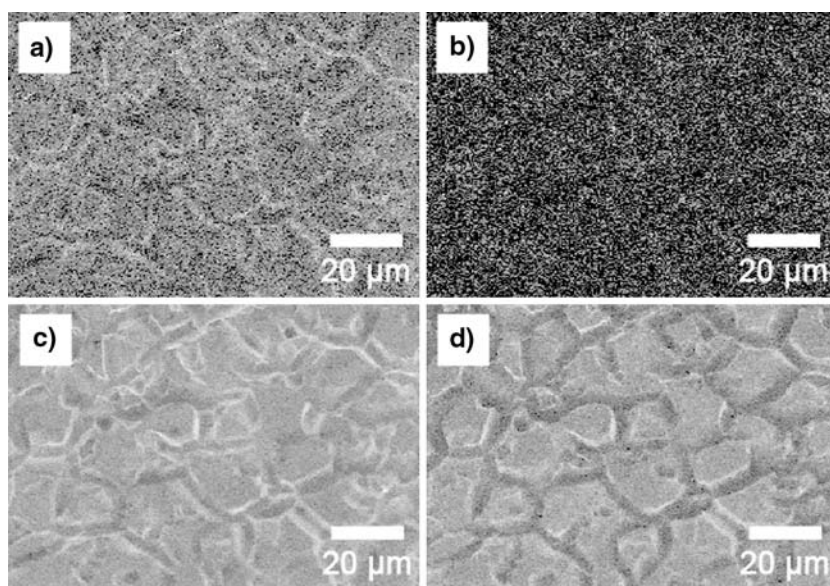
topographic effect is an artefact superimposed on the chemical information. The point measurements on the grain centres and grain boundaries (see Fig. 3) show no difference between the two locations. Comparison with the electropolished reference-stent showed that there is no difference before and after the etching process.

Electrochemical behaviour and metal release

Cyclovoltammetry

In order to study the electrochemical behaviour of the stents in a simulated physiological electrolyte, cyclovoltammetric measurements were performed in Ringer

Fig. 5 (a–d): AES mappings of a stent first etched with nitric and second with oxalic acid with the distribution of the elements iron (a), nickel (b), oxygen (c) and carbon (d). Areas with high concentrations are black and with low concentrations are white in the pictures



solution. With this method it is possible to determine the passivity range of the stents and to study their susceptibility for pitting corrosion. Figure 6 presents the results for all analysed stents. It was not possible to normalize the current obtained with cyclic voltammetry to current density values because the exact area of the stents in the electrolyte could not be determined due to the complex surface morphology and structure. In general, the form of the curves is the same for stents etched in the same electrolyte but with different etching rates. The Flade potentials and breakthrough potentials do not change in the assessed range of etching rates (Fig. 6a–d). Thus no significant differences in the passivation behaviour of stents etched with different etching rates can be observed in the investigated potential range. Differently high currents are measured at the anodic active dissolution peaks in the range of $-600 \text{ mV} < E < -300 \text{ mV}$ and at the anodic breakthrough peaks around $E = +600 \text{ mV}$ for the different etching rates. The reason for this is not clear because as mentioned above no current densities could be calculated and thus it is not possible to compare the different curves quantitatively. Large current spikes (current transients) can be

observed in the CVs in the transpassive range. These current transients indicate local activation and subsequent repassivation (metastable pitting). The material exclusively etched in nitric acid shows the smallest number of current spikes in the transpassive range (Fig. 6a). The highest number of current spikes has been observed for the stents first etched in nitric and secondly in hydrochloric acid (Fig. 6c). These spikes are also visible for the two-step processes with oxalic acid (Fig. 6b) and phosphoric acid (Fig. 6d) used as second solution. The oxidation process of all the stents is irreversible which is indicated by the lower charges of the reduction peak and by the fact that the open circuit potential does not reach its original value after performing one cycle in the cyclic voltammogram.

Figure 7 shows the section of the cyclic voltammograms, which was used for determining the passive range of the stents. The first anodic peak at $-400 \text{ mV} < E < -350 \text{ mV}$ is caused by active dissolution. The Flade potential is the potential at which the passive range begins; it is situated anodic to the active dissolution peak where the current significantly drops. The curves from Figs. 6 and 7 do not show a distinct

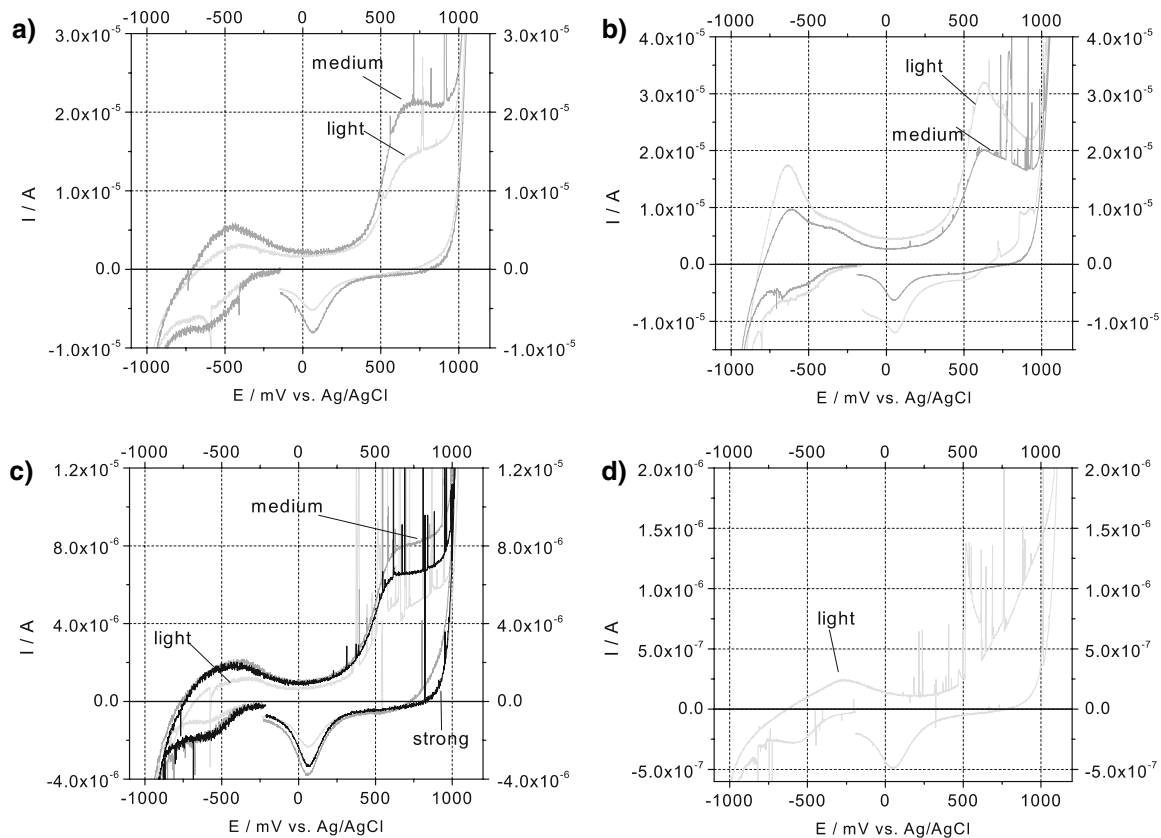


Fig. 6 (a–d): Cyclic voltammograms of stents in Ringer solution etched at room temperature with nitric acid only (a), first with nitric acid and second with oxalic acid (b), second with

hydrochloric acid (c), second with phosphoric acid (d). A light grey line indicates light etching, a grey line medium etching and a black line strong etching. Scanrate = 1 mV/s

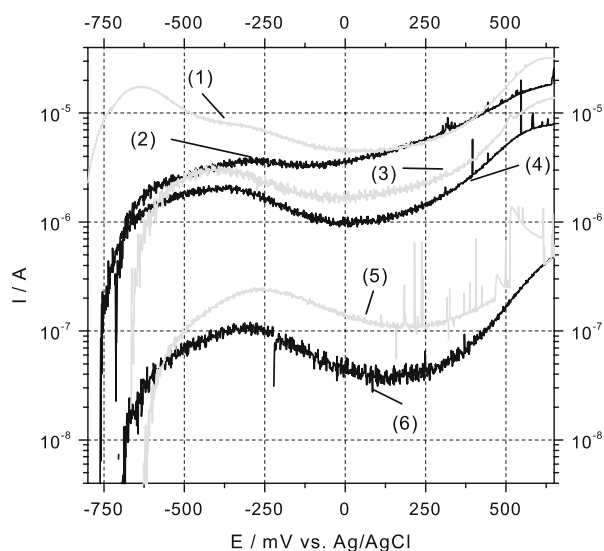


Fig. 7 Cyclic voltammograms at a scan rate of 1 mV/s at room temperature for the stents from Fig. 1: Nitric/oxalic acid (1), sandblasted (2), only nitric acid (3), nitric/hydrochloric acid (4), nitric/phosphoric acid (5) and electropolished (6)

Flade potential. After the passive range, the current increases again as the transpassive breakthrough starts. The breakthrough potential is the potential at which the current rises significantly with respect to the passive current, which is the lowest current in the passive range. Stents that were two-step etched with nitric acid/phosphoric acid (Fig. 7, curve (5)) and with nitric acid/hydrochloric acid (Fig. 7, curve (4)) have their Flade potential around -200 mV and the breakdown potential around 400 mV. The other stents that were one-step etched with nitric acid (Fig. 7, curve (3)) and two-step etched with nitric acid/phosphoric acid (Fig. 7, curve (5)) show a very similar behaviour. The electropolished stent (Fig. 7, curve (6)) and the sandblasted stent (Fig. 7, curve (2)) also give a similar current-potential curve. The surfaces of these stents are in an unmodified state and were therefore used as references. Curve (1) in Fig. 7 shows the results for a stent etched in nitric acid/oxalic acid. This curve differs from those of all other stents as it has two peaks in the range of active dissolution (one peak at -625 mV and a second shoulder at -350 mV). The number of current spikes is very small for the one-step treatment with nitric acid (Fig. 6a) in comparison to all the others (Fig. 6b–d).

Quantification of metal release with AAS

In order to investigate the release of metal ions from the stents during anodic polarization, potentiostatic experiments were performed at $E = 150$ mV above the

respective breakthrough potential, for this purpose it is defined as the potential in the transpassive range where the current has risen again to two times the value of the minimal passive current. The potential was applied for 72 h in every experiment. The current was measured throughout the anodization process and no remarkable current increase or current transients could be detected over the whole time range, which indicates that no stable and no significant metastable pitting corrosion reaction occurred at the applied potential. All experiments were performed in air due to a special experimental set-up that did not allow for providing a nitrogen blanket as protecting atmosphere. This does most likely not hamper the accuracy of the measurement, as the oxidation state of the released metal ions is of no relevance for the detection with AAS. After the potentiostatic experiments the samples were investigated with SEM. The grade of the corrosive attack can be seen in the images of Fig. 8. All stents show at least some surface changes. In case of the electropolished stent the edge of the electrolyte solution in which the stent was immersed is visible (Fig. 8a). The visible surface structures are not grain-boundaries in this case, as the grain size is larger than the features observed and the grains should have a rather hexagonal form. The stent etched with hydrochloric acid shows a high degree of attack (Fig. 8b). Furthermore, precipitates are visible on the surface. These may result from non-soluble salts of corrosion products and the Ringer solution used as electrolyte. Obviously, parts of the stent material only etched with nitric acid dissolved during the experiment (Fig. 8c). The stent etched with nitric acid/oxalic acid shows little corrosion attack and some precipitates (Fig. 8d). Figure 9 depicts the release of nickel and chromium during the experiments. The values are determined by measuring the nickel (Fig. 9a) and chromium (Fig. 9b) concentration of the electrolyte solutions used in the respective dissolution experiments with atomic absorption spectroscopy (AAS). One stent was analysed for each etching method. The black lines indicate the detection limits for the respective experiment. For reference, the pure Ringer solution was analysed with AAS and no nickel or chromium could be detected. The electropolished stent used as reference does not show any detectable nickel or chromium release. The stents etched with nitric and then with hydrochloric acid show the highest value for released nickel. The only sample that showed chromium release was the stent just etched with nitric acid. Thus, the stent etched in a two-step process with nitric acid/oxalic acid shows the lowest heavy metal release compared to all other stents.

Fig. 8 (a–d): SEM pictures taken after potentiostatic corrosion experiments 150 mV above the breakdown potential of an electropolished stent (a), a stent first etched with nitric acid and second with hydrochloric acid (b), a stent only etched with nitric acid (c) and a stent secondly etched with oxalic acid (d)

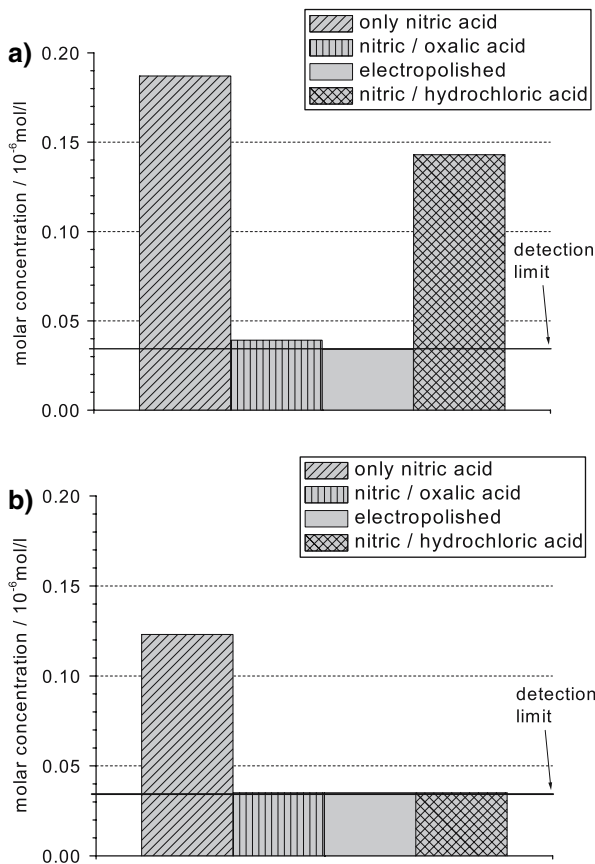
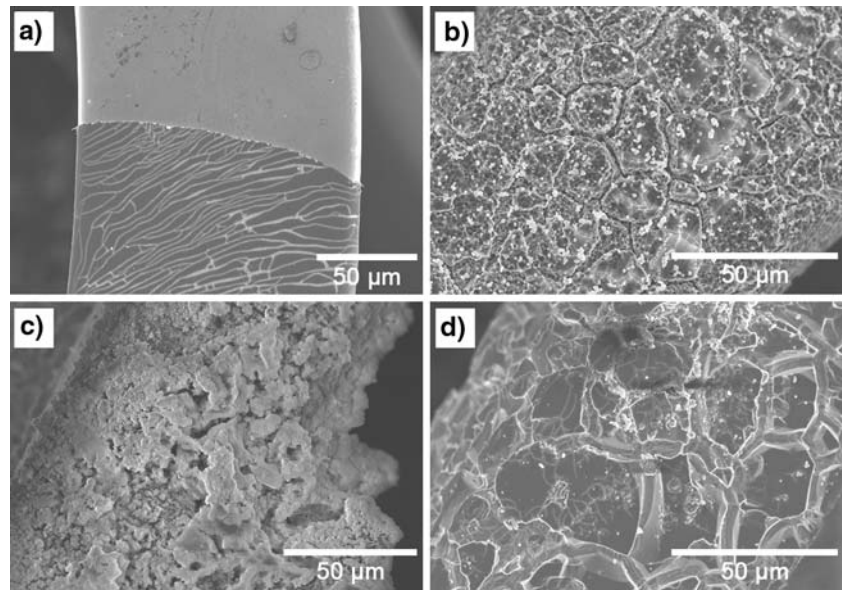


Fig. 9 (a–b): Release of heavy metal ions in the potentiostatic corrosion experiments after 72 h at 150 mV above the breakdown potential. Given is the molar concentration of nickel (a) and chromium (b) in Ringer solution for stents, only etched in nitric acid (diagonally hatched column), first etched in nitric acid and secondly in oxalic acid (vertically etched column), secondly etched in hydrochloric acid (cross-hatched column) and for the electropolished stents as reference (grey column)

Discussion

Analysis of the surface morphology has shown that varying the conditions applied for grain-boundary etching of stainless steel stents can produce very different structures. In order to use the surface structure as drug carrier, there should be a large specific surface area for the storage of drugs. In the mammalian heart the stent is loaded with an oscillating force due to the heart beat; consequently the stent must be fatigue resistant beside the optimal drug elution properties, but sharp edges in the surface morphology will lead to early formation of crevices and fatigue failure as the edges act as notches. A one-step etching with nitric acid seems to form morphologies that are not optimally suited for the situation described above. Two-step combination etching processes yield much better results due to a smoothing of the structures.

Surface analysis with EDX did not show any significant differences in the chemical composition of the differently treated stents. There was also no detectable difference in surface composition at different sites on each stent being grain centres and grain boundaries. The results for the grain boundaries show a large standard deviation and the values are different for differently treated stents. These findings are most likely due to edge effects that occur preferentially when signals from grain-boundaries are detected, as they are not “open” to the detector. As a result those signals coming from the grain-boundaries cannot really be counted as reliable information.

It is not reasonable to use EDX in case of passive layers on steels that develop in air because the information depth of EDX is some microns. But as we are dealing with a corrosion process, there might be a much thicker corrosion layer developing on the material during the grain-boundary etching procedure. In contrast to standard passive films that have a thickness of some nanometres, such corrosion layers might be some microns thick. Therefore from the EDX data it can only be concluded that no corrosion product layer with a thickness of substantially more than some nanometres is formed on the surface during the etching process. However, the composition of the uppermost surface might be changed by the etching treatment.

In contrast to EDX, AES can analyse the uppermost surface oxide layer with a much better sensitivity and lateral resolution. It can be clearly seen from the AES results that the oxide layer has another composition than the bulk material, as it is well known for passive layers on stainless steel. However, the composition of the oxide layer is the same for the analysed two-step etching treatment with nitric acid/oxalic acid, and the as-received electropolished reference stent. These results from Auger spectroscopy indicate that the etching process itself does not cause a change in the surface oxide layer, even though it is possible that a change in the grain boundaries cannot be detected due to the topographical effects explained in the section 3.1. Several authors have analysed the oxide layer of 316L stainless steel for medical applications. In [14] the oxide layer composition of as-produced stainless steel stents (wire coils) with untreated surfaces is examined with AES, a Fe/Ni-ratio of 2.7 and a Fe/Cr-ratio of 1.75 is measured. The surface layer composition after electropolishing has been investigated in [15], XPS measurements showed that the Fe/Cr-ratio of the original surface was 1.31 and after electropolishing the Fe/Cr-ratio was found to be 0.45. In [16] the oxide layer composition is measured under in vivo conditions with AES, here a Fe/Ni-ratio of 4.0 and a Fe/Cr-ratio of 1.28 is found. The comparison of these results shows that the surface oxide layer always has, as expected, a composition different from the one of the bulk alloy. However, the differently treated specimens show quite different compositions of the passive films.

In the present study, neither EDX nor AES studies could indicate clear differences between the chemical composition of the grain boundary region and the grain centre parts. For the etched samples the analysis is hampered by the roughness of the surface. However, even for the electropolished sample such compositional differences could not be detected. Therefore, the strong selective etching of the grain boundaries cannot

be directly attributed to chemical effects. The selective etching is most likely caused by imperfections of the crystal structure at the grain boundaries where the symmetry of the homogeneous crystals is broken. These areas have a higher surface energy than the single crystalline homogeneous surface area inside the grain. Due to that, the grain boundaries are less stable and stronger corrosion attack leads to faster dissolution.

Corrosion resistance is clearly influenced by the etching processes, as indicated by the electrochemical results. The cyclic voltammetry demonstrates that irreversible electrochemical reactions are taking place in the system. The general shape (Fig. 6a–d) of the current voltage curves (CVs) is similar to that reported previously in the literature for Fe-Cr alloy in a near-neutral solution (see e.g. reference [17]). Therefore, the first anodic peak can be ascribed to passivation of the surface; the second anodic peak may be due to oxidation of Cr(III)-species in the passive film into Cr(VI)-species. The potential region of the occurrence of this oxidation peak is in accordance with the electrochemical behaviour of pure chromium [18] as well as observations in the literature concerning transpassive dissolution of Cr and Fe-Cr oxide films (see e.g. [19, 20] and references therein).

The passivation behaviour is very similar for all stents. Only the stent two-step etched with nitric/oxalic acid shows a different behaviour. The peak of active dissolution shows two different maxima. The first larger peak at around $E = -650$ mV should result from the fact that the surface of this stent was more active than those of the other stents. The second smaller shoulder at around $E = -300$ mV_{Ag/AgCl} is in the same range as the active dissolution peak of all other etchants. So this shoulder is most likely the beginning of the passive range, which means that the passive range is similar to the other examined stents.

Current spikes were detected in the transpassive range; these spikes are most likely caused by metastable pitting corrosion. In general, more spikes were detected upon analysis of stents etched in a two-step process. This leads to the assumption that the two-step processes have a higher risk of inducing pitting corrosion events. It is surprising that not only etching with hydrochloric acid but also with oxalic acid, for example, leads to pitting corrosion. The stents etched with hydrochloric acid as second electrolyte have the most spikes. This could be due to chloride ions that are trapped in the grain boundary trenches after the etching treatments. The morphology also influences the pitting behaviour. This might be one reason for the spikes observed in the experiments with nitric/oxalic acid.

Long-time anodic polarization experiments lead to a strong attack of the surface, except for the two-step nitric/oxalic acid etched stent. In all cases precipitates of corrosion products are present on the surface. Regarding heavy metal release, the etching process with nitric acid and oxalic acid gives the best results. However, since only one stent was used for each measurement the statistical relevance of the results should still be verified.

In summary, the stents etched with nitric/oxalic acid show the least attack and least metal ion release in long-term polarization in the transpassive region, and moreover a similar passive behaviour to all the other stents in the cyclic voltammetry experiments. Further, the morphology of the stents etched with nitric/oxalic acid is optimal. Thus, the stents two-step etched with nitric/oxalic acid are the ones that are most suited for an application in the human body with respect to corrosion stability.

Summary and conclusions

Stainless steel stents treated by a two-step etching procedure with nitric/oxalic acid give the best results in the described corrosion resistance studies in that

- (i) the in-vitro-elution of chromium and nickel at transpassive potentials is lowest for these stents, and
- (ii) the passive region is similar to all other stents. Additionally, the morphology is optimal in respect to other stent properties, especially mechanical fatigue resistance.

For all two-step etched stents the risk of pitting corrosion may be larger than for one-step etched stents, as shown by spikes in the cyclovoltammetry in the passive range which indicate local activation/repassivation events taking place. Nevertheless, the one-step etching process did not lead to an applicable result with respect to corrosion resistance, as the release of heavy metal ions was much higher than for all other stents at transpassive potentials, which means that the stent could be less biocompatible due to metal ion release in the body. The risk of pitting corrosion has to be considered for the development of electrochemical etching methods for 316L.

A surface sensitive Auger analysis revealed that the composition of the passive film was not changed by the etching treatment as compared with electro-polished surface, not even in the grain-boundary area.

The aim of the present study was to describe the corrosion properties of new drug-eluting stents. The drug elution itself was not examined. For application in the human body, both drug elution as well as corrosion resistance have to be considered as one is determining the pharmaceutical properties and the other, beside biological aspects, the biocompatibility of the implant. Some optimisation will be possible by adjusting the exact etching process parameters.

Acknowledgments The authors gratefully acknowledge the Bayerische Forschungsstiftung (BFS) and the Deutsche Forschungsgemeinschaft (DFG) for the financial support and Helga Hildebrand as well as Anja Friedrich for performing the surface analytical SEM and AES measurements.

References

1. EUROPEAN COMMISSION, In “*The Health Status of the European Union*” (European Communities, Luxembourg: 2003), p. 11
2. B. HEUBLEIN, *Prog. Biomed. Res.* **4** (1999) 1
3. P. P. LEIMGRUBER, G. S. ROUBIN, J. HOLLMAN, G. A. COTSONIS, B. MEIER, J. S. DOUGLAS, S. B. KING, A. R. GRUENTZIG, *Circulation* **73** (1986) 710
4. M. R. BELL, P. B. BERGER, J. F. BRESNAHAN, G. S. REEDER, K. R. BAILEY, D. R. HOLMES, *Circulation* **85** (1992) 1003
5. S. L. GOLDBERG, A. LOUSSARARIAN, J. DE GREGORIO, C. DI MARIO, R. ALBIERO, A. COLOMBO, *J. Am. Coll. Cardiol.* **37** (2001) 1019
6. R. HOFFMANN, G. S. MINTZ, G. R. DUSSAILLANT, J. J. POPMA, A. D. PICHARD, L. F. SATLER, K. M. KENT, J. GRIFFIN, M. B. LEON, *Circulation* **94** (1996) 1247
7. D. R. HOLMES, *Am. J. Cardiol.* **91** (2003) 50A
8. P. W. SERRUYS, E. REGAR, A. J. CARTER, *Heart* **87** (2002) 305
9. R. FATTORI, T. PIVA, *Lancet* **361** (2003) 247
10. M. STÖVER, M. RENKE-GLUSZKO, T. SCHRATZENSTALLER, J. WILL, N. KLINK, B. BEHNISCH, A. KASTRATI, R. WESSELY, J. HAUSLEITER, A. SCHÖMIG and E. WINTERMANTEL, *J. Mater. Sci.* **41** (2006) 5569
11. F. C. BELL, D. E. SONON, *Metallography* **9** (1976) 91
12. A. J. SEDRIKS, In “*Corrosion of stainless steels*” (Wiley, New York: 1996)
13. Z. SZLARSKA-SMIALOWSKA, In “*Pitting corrosion of metals*” (NACE, Houston, 1986)
14. C.-C. SHIH, C.-M. SHIH, Y.-Y. SU, M.-S. CHANG, S.-J. LIN, *Appl. Surf. Sci.* **219** (2003) 347
15. S.-J. LEE, J.-J. LAI, *J. Mat. Proc. Tech.* **140** (2003) 206
16. R. A. SILVA, M. A. BARBOSA, G. M. JENKINS, I. SUTHERLAND, *Biomaterials* **11** (1990) 336
17. S. VIRTANEN, M. BÜCHLER, *Corr. Sci.* **45** (2003) 1405
18. M. POURBAIX, In “*Atlas of Electrochemical Equilibria in Aqueous Solutions*” (NACE, Houston: 1974)
19. P. SCHMUKI S. VIRTANEN A. J. DAVENPORT C. M. VITUS, *J. Electrochem. Soc.* **143** (1996) 3997
20. P. SCHMUKI, S. VIRTANEN, H. S. ISAACS, M. P. RYAN, A. J. DAVENPORT, H. BÖHNI, T. STENBERG, *J. Electrochem. Soc.* **145** (1998) 791